Int J Mater Form (2009) Vol. 2 Suppl 1:315–318
DOI 10.1007/s12289-009-0662-y

MODELING OF FRICTION STIR PROCESSING USING 3D CFD ANALYSIS

S.Z. Aljoaba[1], I.S Jawahir[1], O.W Dillon Jr[1]., M.H. Ali[1], M.K. Khraisheh[1*]

[1]Center for Manufacturing and Mechanical Engineering Department, University of Kentucky, USA
[*]Masdar Institute of Science and Technology, Abu Dhabi, United Arab Emirates

ABSTRACT: Friction Stir Processing (FSP) has emerged as an effective tool for enhancing sheet metal properties through microstructural modification of processed materials. Despite the large number of studies, most of the work that has been done in the FSP field focuses primarily on experimental work. Only limited modeling attempts on temperature distribution and strain rate analysis have been conducted. In this work, a three dimensional Computational Fluid Dynamics (CFD) model was developed to simulate FSP using the STAR CCM+ CFD commercial software. User-defined subroutines were developed and implemented to investigate the effects of process parameters on temperature, strain rate, flow stress and material velocity fields in, and around, the processed nugget. In addition, a correlation between process parameters and the Zener-Holloman parameter was developed to predict the grain size distribution in the processed zone. Different stirring conditions were incorporated in this study to investigate their effects on material flow and microstructural modification. The modeling results were compared with the available experimental data and showed good agreement.

KEYWORDS: FSP, Computational Fluid Dynamics, Temperature, Grain size, Strain rate, Dynamic viscosity.

1 INTRODUCTION

On observing the advantages associated with friction stir welding (FSW), mainly grain refinement, the phenomenon has been extended to the processing of commercial alloys. Friction stir processing (FSP) is a solid-state process in which a specially designed rotating cylindrical tool, consisting of a pin and a shoulder, is plunged into the sheet. The tool is then traversed in the desired direction (Figure 1). Several researchers [1-5] used Computational Fluid Dynamics (CFD) to simulate FSP. They assumed the FS processed material to be fluid. They used different CFD codes to determine velocity fields, material flow and temperature distributions. In general, most of the CFD work that has been done to simulate FSP or FSW uses two dimensional models and neglects the dependency of material properties on either temperature, strain rate, or both. Still there is a great need for a comprehensive 3D model which can accurately simulate the actual FSP/FSW process. In this work, a three dimensional CFD model is developed to simulate FSP using the STAR CCM+ CFD commercial software.

2 MODEL DESCRIPTION

The simulation is based on solving continuity, momentum, and energy equations. The model consists of two bodies; the first one is the tool, which is assumed to be a rigid solid body. The second one is the sheet, which is assumed to be liquid while demonstrating actual sheet-material properties. An interface between the tool and the sheet was created, and it was assumed that each point on the interface has the same velocity as its corresponding point on the tool. Several user-defined functions were defined to calculate the dynamic viscosity of the material which is mainly a function of local values of temperature and strain rate.

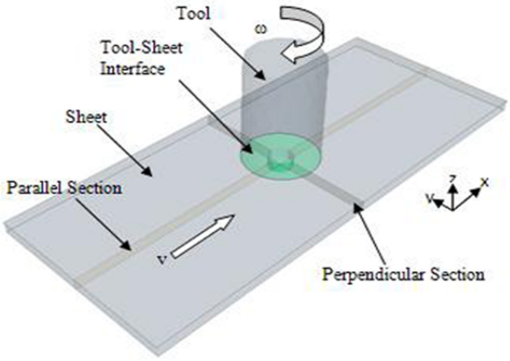

Figure 1: Model's geometry

The following formulations of flow stress, Zener Holloman, and dynamic viscosity were proposed by Sheppared and Wright [6]:

$$\sigma_e = \frac{1}{\alpha} sinh^{-1}\left[\left(\frac{Z}{A}\right)^{1/n}\right] \tag{1}$$

$$Z = \dot{\varepsilon}\ \exp\left(\frac{Q}{RT}\right) \tag{2}$$

$$\mu = \frac{\sigma_e}{3\dot{\varepsilon}} \tag{3}$$

---

*M. K. Khraisheh: Masdar Institute of Science and Technology, Abu Dhabi, UAE, Tel + 971 2 698-8169, Fax + 971 2 698-8121, mkhraisheh@mist.ac.ae

Where A, α, and n are material constants. Z: Zener Holloman constant. Q: activation energy, R: gas constant. $\dot{\varepsilon}$: effective strain rate. μ: dynamic viscosity. The heat generated at the tool/sheet interface was assumed to be a heat flux which is a frictional heat and is given as [7]:

$$Q = 2\pi \mu_f F_n R_i \omega \tag{4}$$

Where R_i: distance from the calculated point to the axis of the rotating tool, ω: rotational speed of the tool, μ_f: coefficient of friction between the tool and the sheet. F_n: normal force. The top and bottom of the sheet were assumed to lose heat to the surroundings through convection. For the sides of the sheet, fixed temperature boundary condition was assumed and was equal to room temperature since the sheet is considered thin.

3 RESULTS AND DISCUSSION

The model was built with a flat tool-pin geometry that has a 6.4mm pin diameter, and 19.1mm shoulder diameter. The material of the sheet is Mg AZ31B-O magnesium alloy with a 3.2mm thickness. The material of the tool is Tool Steel H13. The data used in the analysis are given in Table 1.

3.1 PREDICTED TEMPERATURE FIELDS

The temperature contours were calculated for different stirring conditions. As shown in Figure 2, it was noticed that temperature increased as rotational speed increased. It was also noticed that the temperature of stirred material increased with increasing distance to the tool's outer edge. This is expected; since the material there has higher velocity of deformation due to its position, the velocity is highest at the shoulder's edges, and accordingly, has higher friction and plastic deformation. The contours are shaped like onion rings and are showing a difference in the temperature distribution between zones before and after the tool pin. There was also a small difference between the advancing and the retreating sides. Figure 2.c shows the highest temperature is 1000K, which exceeds the melting point of the material; this is due to the 1720 rpm rotational speed, which was also verified experimentally, where the material melted at these high rotational speeds.

Table 1: Data used in analysis

Properties and constants	Value
Sheet material density[8]	1777 Kg/m^3
Specific heat[8]	$0.2441+105\text{e-}6T-2783T^{-2}$
Thermal Conductivity[8]	96 W/m-K
Liquidus temperature[8]	903 K
Solidus temperature[8]	878 K
Activation Energy Q[9]	130 KJ/mol
Material Constant A[9]	2.75E7 s^{-1}
Material Constant n[9]	1.8
Material Constant α[9]	0.052 MPa^{-1}
Gas Constant R[9]	8.314472 J/K-mol
Tool material density[8]	7800 Kg/m^3
Specific Heat[8]	460 J/Kg-K
Thermal Conductivity[8]	24.3 W/m-K

a.1:Parallel section

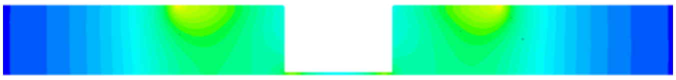

a.2:perpendicular section

b.1:Parallel section

b.2:Perpendicular section

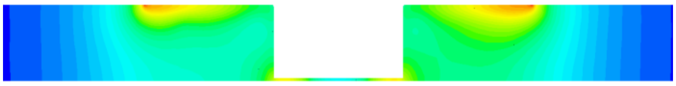

c.1:Parallel section

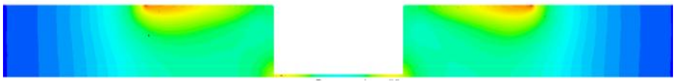

c.2: Perpendicular section

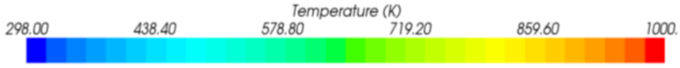

Figure 2: Temperature distribution. a: 1000 rpm, b: 1200 rpm, c:1750 rpm.

3.2 PREDICTED STRAIN RATE VALUES

Strain rate has always been difficult to measure experimentally. The STAR CCM+ tools provide the ability to determine the strain rate during the stirring process. Figure 3 shows the determined strain rate values and its distribution under different conditions. It is noticed that strain rate values are highly affected by the rotational speed, where it increases, strain rate increases. The highest values are at the contact zone with the outer edge of the tool's shoulder, where the temperature and the material speed are the highest.

3.3 PREDICTED DYNAMIC VISCOSITY VALUES

As it can be seen in Figure 4, dynamic viscosity is highly affected by temperature and strain rate. The subroutine that determines the dynamic viscosity is applied only to the processed zone, while an initial value is assumed to be 1E5 Pa.s for the as-received sheets. The results show a reverse relationship between the rotational speed and the dynamic viscosity. It can also be noticed that the dynamic viscosity contours are dissimilar at both sides of the cross sections due to the dissimilar temperature and strain rate values at those zones.

3.4 PREDICTED GRAIN SIZE

Grain size is determined using an empirical relationship (Equation (5)) that relates the Zener Holloman constant to it. The relationship is developed using experimental measurements of the grain size (d in microns) of the processed alloy at the same stirring conditions.

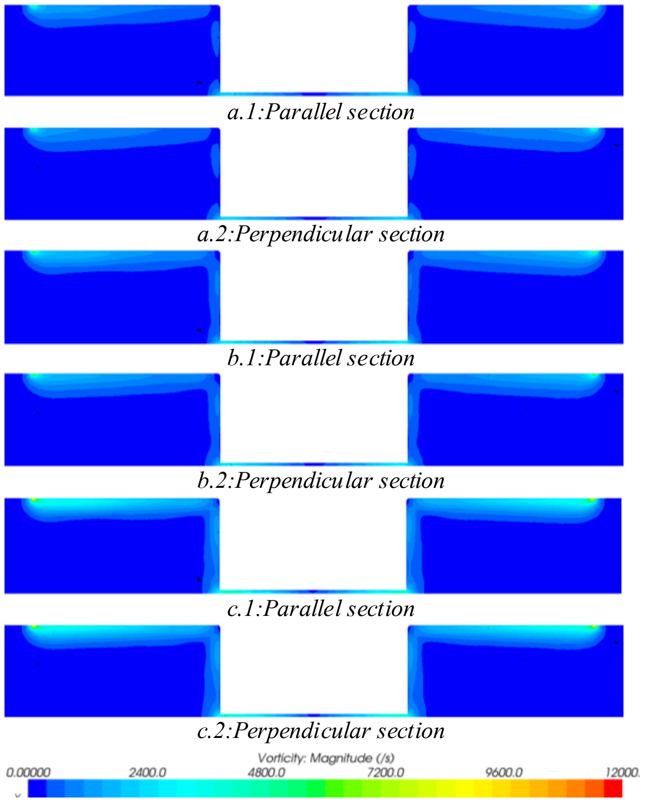

a.1:Parallel section

a.2:Perpendicular section

b.1:Parallel section

b.2:Perpendicular section

c.1:Parallel section

c.2:Perpendicular section

Figure 3: *Strain rate values. a: 1000rpm, b: 1200rpm, c: 1750rpm.*

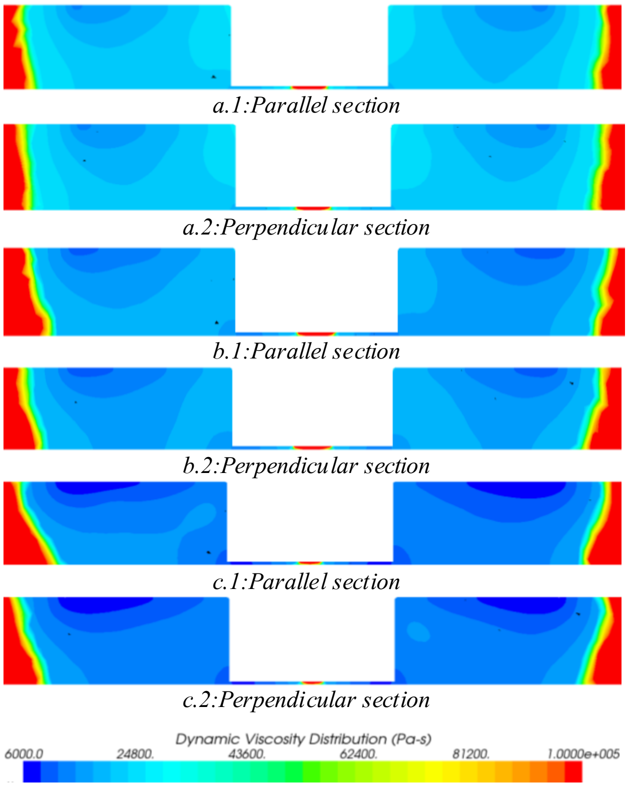

a.1:Parallel section

a.2:Perpendicular section

b.1:Parallel section

b.2:Perpendicular section

c.1:Parallel section

c.2:Perpendicular section

Figure 4: *Dynamic viscosity distribution. a: 1000rpm, b: 1200rpm, c: 1750rpm.*

$$\ln(d) = 8.646 - 0.2104\ln(Z) \qquad (5)$$

Temperature range of the magnesium alloys recrystallization is 523-753K. Figure 5 shows the distribution of the predicted grain size. It is noticed that as the rotational speed increases, the average grain size increases. This is due to the increased temperature. The average grain size at the advancing side of the stirring zone is smaller than that of the retreating side; and in front of the tool is smaller than that at the back side of the tool at that zone. This again supports the dissimilarity in temperature and strain rate distributions at these zones. It can be seen that the average grain size at the top of the processed zone is larger than those at lower levels. This might be due to the higher temperature values at the top, which helps in grain growth. It can be noticed that the average grain size at the shoulder edges is larger than that in other regions in the processed zones. This also can be attributed to the highest values of temperature at such a region. The average grain size values that were obtained were close to the experimental results that were presented by Darras [10].

3.5 PREDICTED MATERIAL VELOCITY FIELDS

Figure 6 shows the velocity fields within the parallel and perpendicular sections along the sheet at the FS processed zone. It can be noticed that the velocity of the material increases as the rotational speed increases. Furthermore, velocity fields were dissimilar in all directions around the tool. It can be obtained that the material does not move by the same speed or same directions. The highest speed values are for the material that is in contact with the outer edge of the tool's shoulder; this is due to the fact that the tangential velocity is directly proportional to the radius which is of highest value at the edge.

4. CONCLUSIONS

Friction stir processing is an effective microstructural modification process that produces a finer and more homogenous grain structure. Specifying the tool geometry and the stirring conditions (rotational and translational speeds) are important issues in FSP in order to obtain the desired grain refinement. The temperature is highly effective factor influencing the grain size, and is highly affected by the stirring conditions. CFD represents a useful tool to simulate the FSP that provides a good estimate for the material behavior during the process. It also provides results that are close to those obtained experimentally if all conditions and assumptions are provided properly. It can be used also to predict physical quantities that are difficult to measure. It can also estimate strain rate, and material velocity values and directions. CFD can be used to predict the material flow, which will be one of the challenging issues that will lead to optimum tool geometry designs to obtain fine grains using high rotational speeds.

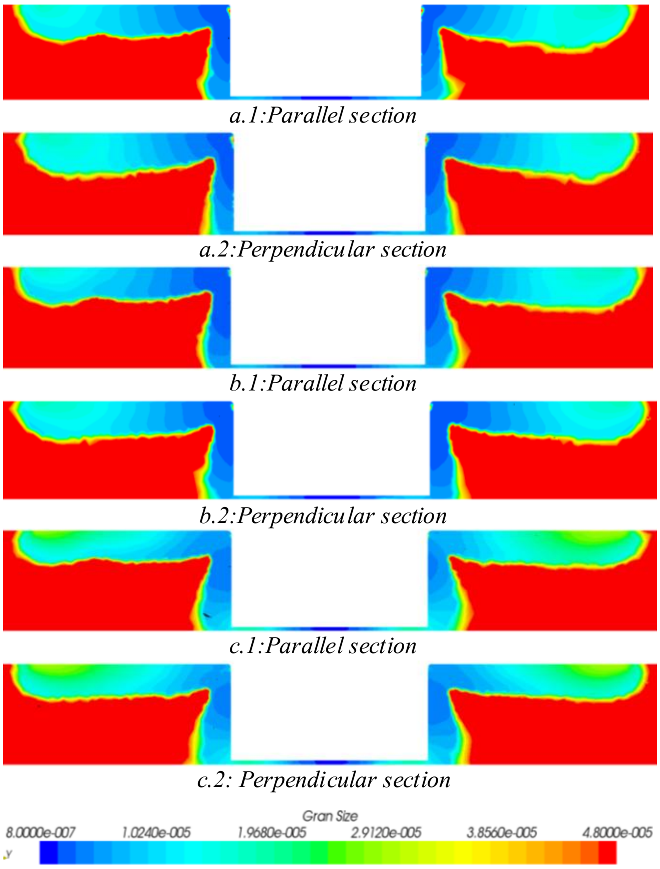
a.1:Parallel section

a.2:Perpendicular section

b.1:Parallel section

b.2:Perpendicular section

c.1:Parallel section

c.2: Perpendicular section

Figure 5: Grain size distribution. a: 1000rpm, b: 1200rpm, c: 1750rpm.

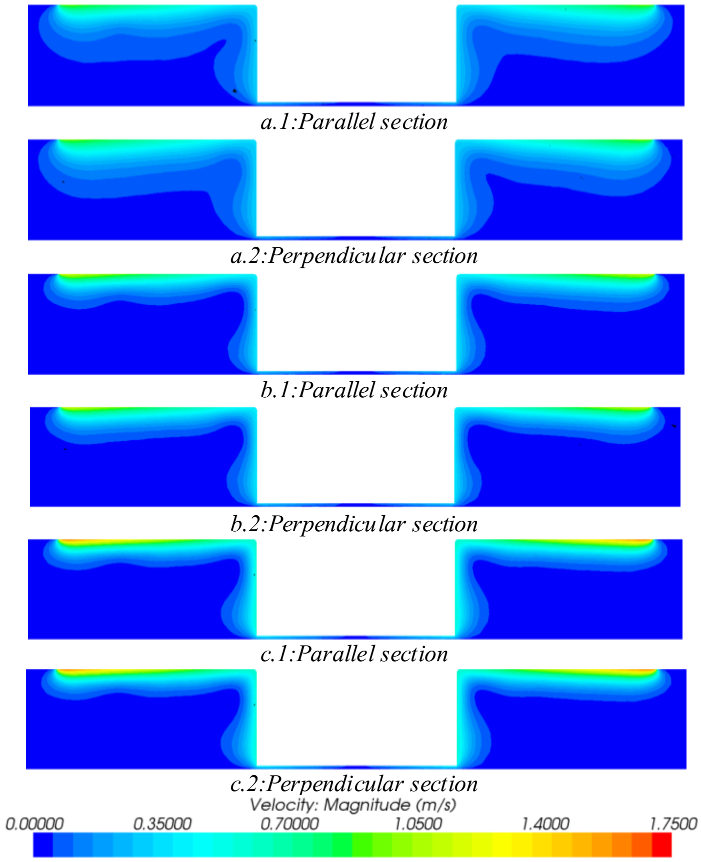
a.1:Parallel section

a.2:Perpendicular section

b.1:Parallel section

b.2:Perpendicular section

c.1:Parallel section

c.2:Perpendicular section

Figure 6: Velocity fields. a: 1000rpm, b: 1200rpm, c: 1750rpm.

5. ACKNOWLEDGMENT

The support of Integrated Manufacturing Technology Initiative (IMTI) is acknowledged.

6. REFERENCES

[1] P. Colegrove , Hugh R. Shercliff: **3-Dimensional CFD modeling of flow round a threaded friction stir welding tool profile**, Materials Processing Technology , 169: 320–327, 2005.

[2] T. Hyoe, P.A. Colegrove, H.R. Shercliff: **Thermal And Microstructure Modeling in Thick Plate Aluminum Alloy 7075 Friction Stir Welds**, *Friction Stir Welding and Processing II, TMS (The Minerals, Metals & Materials Society),* 2003.

[3] H. Schmidt and J. Hattel: CFD modeling of the shear layer around the tool probe in friction stir welding, In: *Friction Stir and Processing III*, TMS, pages 225-232, 2005.

[4] P. Colegrove and H. Sherchiff, 2-Dimensional CFD modeling of flow round profiled FSW tooling, In: *Friction Stir Welding and Processing II*, TMS, pages 13-23, 2003.

[5] Tianzhong Long, Tilman Urs Seidel, Wei Tang, and Anthony P. Reynolds: A Friction Stir Welding Model Using Computational Fluid Dynamics, In: *Hot Deformation of Aluminum Alloys III, TMS Annual Meeting*, San Diego, CA, 299-312, 2003.

[6] T. Sheppard and D.S. Wright: *Metal. Technology*, 1979, 6:215-223.

[7] Song, M. and Kovacivic: **R. Numerical and experimental study of heat transfer process in friction stir welding**. Proc. Instn Mech. Engrs, Part B: J. Engineering Manufacture, 217(B1): 73-85, 2003.

[8] ASM Handbook, **ASM International Metals Handbook**, Tenth Edition, 2: 455, 1990.

[9] H.J. McQueen, M. Myshlaev, M. Sauerborn and A. Mwembela: Flow Stress Microstructures And Modeling In Hot Extrusions Of Magnesium Alloys, In: *Magnesium Technology 2000*, *The Minerals, Metals and Materials Society*, pages 355-362, 2000.

[10] Darras B., **Integrated thermo-mechanical investigations of friction stir processing of light weight alloys**, PH.D Theses, University of Kentucky, Lexington, KY, US, p.47, 2008.